

## THE DIFFUSE EMISSION AND A VARIABLE ULX IN THE ELLIPTICAL GALAXY NGC 3379

LAURENCE P. DAVID, CHRISTINE JONES, WILLIAM FORMAN &amp; STEVE MURRAY

Harvard-Smithsonian Center for Astrophysics, 60 Garden St., Cambridge, MA 02138;

david@cfa.harvard.edu

*submitted to The Astrophysical Journal*

## ABSTRACT

A Chandra observation of the intermediate luminosity ( $M_B = -20$ ) elliptical galaxy NGC 3379 resolves 75% of the X-ray emission within the central 5 kpc into point sources. Spectral analysis of the remaining unresolved emission within the central 770 pc indicates that 90% of the emission probably arises from undetected point sources, while 10% arises from thermal emission from  $kT = 0.6$  keV gas. Assuming a uniform density distribution in the central region of the galaxy gives a gas mass of  $5 \times 10^5 M_\odot$ . Such a small amount of gas can be supplied by stellar mass loss in only  $10^7$  years. Thus, the gas must be accreting into the central supermassive black hole at a very low radiative efficiency as in the ADAF or RIAF models, or is being expelled in a galactic wind driven by the same AGN feedback mechanism as that observed in cluster cooling flows. If the gas is being expelled in an AGN driven wind, then the ratio of mechanical to radio power of the AGN must be  $10^4$ , which is comparable to that measured in cluster cooling flows which have recently been perturbed by radio outbursts. Only 8% of the detected point sources are coincident with globular cluster positions, which is significantly less than that found among other ellipticals observed by Chandra. The low specific frequency of globular clusters and the small fraction of X-ray point sources associated with globulars in NGC 3379 is more similar to the properties of lenticular galaxies rather than ellipticals.

The brightest point source in NGC 3379 is located 360 pc from the central AGN with a peak luminosity of  $3.5 \times 10^{39}$  ergs  $s^{-1}$ , which places it in the class of ultra-luminous X-ray point sources (ULX). Analysis of an archival ROSAT HRI observation of NGC 3379 shows that this source was at a comparable luminosity 5 years prior to the Chandra observation. The spectrum of the ULX is well described by a power-law model with  $\Gamma = 1.6 \pm 0.3$  and galactic absorption, similar to other ULXs observed by Chandra and XMM-Newton and to the low-hard state observed in galactic black hole binaries. During the Chandra observation, the source intensity smoothly varies by a factor of two with the suggestion of an 8-10 hour period. No changes in hardness ratio are detected as the intensity of the source varies. While periodic behavior has recently been detected in several ULXs, all of these reside within spiral galaxies. The ULX in NGC 3379 is the only known ULX in an elliptical galaxy with a smoothly varying light curve suggestive of an eclipsing binary system.

*Subject headings:* binaries:close – galaxies:elliptical and lenticular – galaxies:ISM – galaxies:individual (NGC 3379) – X-ray:binaries – X-ray:galaxies – X-ray:ISM

## 1. INTRODUCTION

Einstein observations showed that the bulk of the X-ray emission from optically luminous early-type galaxies arises from hot gas in hydrostatic equilibrium (Forman, Jones & Tucker 1985). A spectrally harder X-ray component, more prevalent among low luminosity ellipticals, was detected by ASCA and assumed to arise from low-mass X-ray binaries (LMXBs) due to the old stellar population in these galaxies (Kim, Fabbiano & Trinchieri 1992). Chandra, with its superior angular resolution, has resolved populations of point sources in many early-type galaxies (e.g., Angelini, Lowenstein & Mushotzky 2001; Sarazin, Irwin & Bregman 2001; Kraft et al. 2001; Blanton, Sarazin & Irwin 2001; Finogeev & Jones 2002, Jeltema et al. 2003). Between 20 and 80% of the point sources detected in early-type galaxies reside in globular clusters (Sarazin et al. 2003). This is consistent with observations of our own galaxy which show that LMXBs are preferentially located in globular clusters compared to the rest of the galaxy (White, Nagase & Van den Heuvel 1995).

Ultra-luminous X-ray point sources (ULXs), off-nuclear point sources with  $L_x \gtrsim 10^{39}$  ergs  $s^{-1}$ , have been reported in approximately 15 early-type galaxies (e.g., Angelini et al. 2001; Sarazin, Irwin & Bregman 2001; Jeltema et al. 2003; Swartz et al. 2004). However, Irwin, Bregman & Athey (2004) ar-

gue that the statistics of ULXs in early-type galaxies with  $L_x > 2 \times 10^{39}$  ergs  $s^{-1}$  are consistent with background sources. Swartz et al. (2004) analyzed archival Chandra observations of 82 galaxies and compiled a sample of 154 ULXs. They list two ULXs in NGC 3379 and also report that the the most luminous source is likely variable. The minimum luminosity for an ULX corresponds to the Eddington luminosity of the most massive black holes expected to form from stellar core collapse (Fryer & Kalogera 2001). The nature and origin of ULXs are unknown, but they could arise from non-isotropic emission from stellar mass black holes (King et al. 2001), super-Eddington emission from stellar mass black holes with inhomogeneous disks (Begelman 2002), or sub-Eddington emission from intermediate mass black holes (IMBHs).

NGC 3379 is an intermediate luminosity ( $M_B = -20.0$ ) E1 galaxy in the Leo I group at a distance of 10.6 Mpc (Tonry et al. 2001). The large scale optical morphology of NCG3379 is nearly featureless and well fitted with a de Vaucouleurs profile (Capaccioli et al. 1990). Terlevich & Forbes (2002) estimate a stellar age of 9.3 Gyr for NGC 3379. Both of these characteristics indicate that NGC 3379 has not undergone a major merger in the recent past. However, warm ionized gas and dust have been detected in the central few arcseconds of NGC 3379

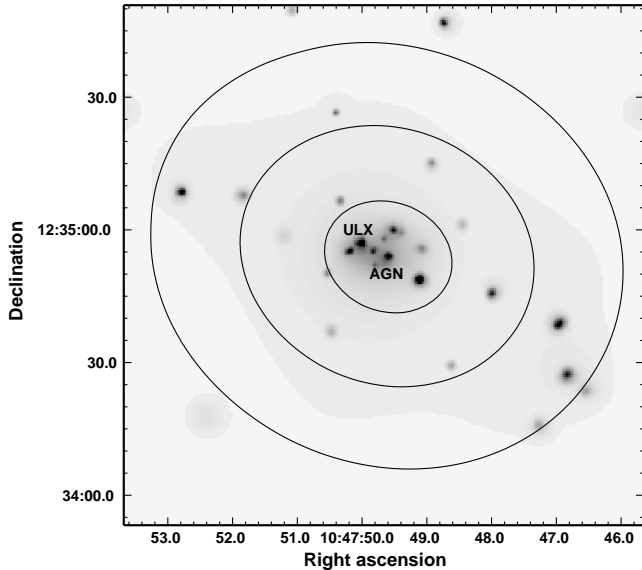


FIG. 1.— Adaptively smoothed 0.3-6.0 keV ACIS-S3 image of the central  $2'$  by  $2'$  (6.2 kpc) region of NGC 3379 along with the optical isophotes of the galaxy. The AGN at the galactic center and the ULX are labeled.

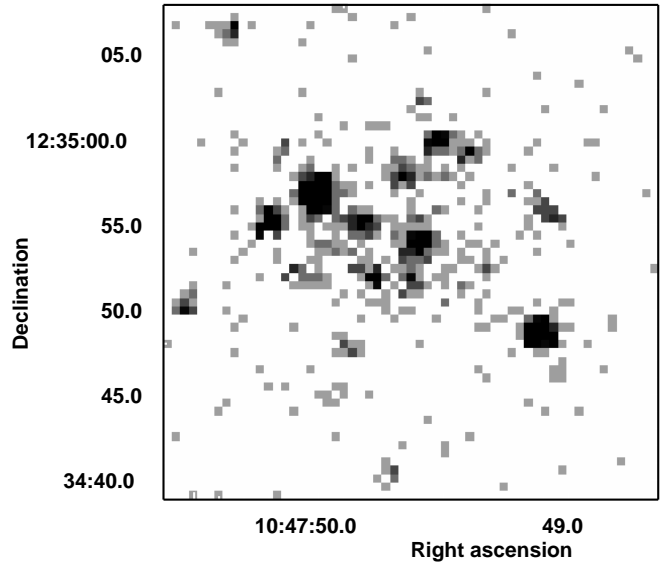


FIG. 2.— Raw 0.3-6.0 keV ACIS-S3 image of the central  $30''$  by  $30''$  (1.5 kpc) region of NGC 3379.

(Macchetto et al. 1996, van Dokkum & Franx 1995). Statler (2001) argues that the  $1.5''$  (77 pc) dust ring is dynamically decoupled from the stars and likely has an external origin. There is also some evidence for a central stellar disk based on the stellar rotation curves (Pastoriza et al. 2000) along with a central compact object with a mass of  $1.0 - 3.9 \times 10^8 M_{\odot}$  (Magorrian et al. 1998, Haring & Rix 2004). Thus, while the outer regions of NGC 3379 are dynamically relaxed, there are some indications of recent merger activity in the central parts of the galaxy.

In §2 we discuss the general properties of the X-ray point population detected in the Chandra observation of NGC 3379, including the luminosity function, spatial distribution and hardness ratios. In §3 we discuss the spectral and temporal characteristics of the ULX.

The properties of the diffuse emission and the central AGN are presented in §4. A discussion concerning the nature of the ULX and the dynamic state of the hot gas in NGC 3379 is given in §5, followed by a brief summary of our main results in §6.

## 2. THE POINT SOURCE POPULATION

NGC 3379 was observed by Chandra for 33,744 s on Feb. 13, 2001 with the ACIS-S detector in faint telemetry mode. The data were reprocessed with the CIAO 3.2 version of *acis\_process\_events* along with CALDB 3.0. Filtering the S3 data for background flares leaves 31,199 s of cleaned data. Since the archived data were processed several years ago, we also followed the *fix off-sets* thread on the CXC web pages to improve the astrometry, but this only produced a shift of  $0.12''$ . We then checked for X-ray detections of stars in the USNO-B1.0 catalog and found one star with an optical position off-set by  $0.2''$  from its X-ray position, which is within the absolute astrometry uncertainties of Chandra and the USNO B1 catalog.

An adaptively smoothed 0.3-6.0 keV S3 image of the central  $2'$  by  $2'$  region (6.2 kpc on a side) is shown in Fig. 1 along with the optical isophotes of the galaxy. This image shows that most of the X-ray emission from NGC 3379 is resolved by Chandra into point sources, many of which are aligned along the major optical axis of the galaxy. The point source labeled AGN in Fig.

1 is located within  $1''$  of the optical centroid of the galaxy, and is probably associated with the central supermassive black hole with a dynamically measured mass of  $1.0 - 3.9 \times 10^8 M_{\odot}$  (Magorrian et al. 1998, Haring & Rix 2004). The brightest source in NGC 3379 (labeled ULX in Fig. 1) is located  $7''$  (360 pc) to the NE of the AGN. The center of NGC 3379 has a high surface density of point sources, as can be seen in the full resolution, raw data image of the central  $30''$  by  $30''$  (1.5 kpc) region shown in Fig. 2.

Using a wavelet detection algorithm on the 0.3-6.0 keV image with a detection threshold of  $10^{-6}$ , we detect 66 sources within the S3 field of view. The point source detection sensitivity varies across the field of view due to the presence of extended emission in the center of the galaxy with an average, exposure-corrected  $3\sigma$  threshold of  $3.1 \times 10^{-4}$  ct  $s^{-1}$ . Assuming an absorbed power-law model with galactic absorption ( $N_H = 2.79 \times 10^{20}$   $cm^{-2}$ ) and index  $\Gamma = 1.7$ , this count rate corresponds to an unabsorbed 0.3-10.0 keV flux of  $1.6 \times 10^{-15}$  ergs  $cm^{-2}$   $s^{-1}$  and luminosity  $L(0.3-10.0 \text{ keV}) = 2.2 \times 10^{37}$  ergs  $s^{-1}$ . Forty sources above this threshold are detected in the central  $1.6'$  (5 kpc). Based on the Chandra deep field south (Giacconi et al. 2001), approximately one of these sources is likely a background object. Beyond 5 kpc, approximately 7 of the detected 26 sources are likely background objects. We therefore restrict most analysis to the central 5 kpc of the galaxy.

Based on our count rate conversion factor, the two brightest sources in NGC 3379 have luminosities of  $2.4 \times 10^{39}$  ergs  $s^{-1}$  and  $6.8 \times 10^{38}$  ergs  $s^{-1}$ . The luminosity of the brightest source is consistent with that obtained by Swartz et al. (2004), but the luminosity of the second brightest source is a factor of 1.8 less than that given by Swartz et al., after correcting for the slightly larger distance used by Swartz et al. of 11.1 Mpc from Ferrarese et al. (2000). Swartz et al. derived unabsorbed X-ray fluxes in the 0.5-8.0 keV band pass by fitting an absorbed power-law model to the spectra of each candidate ULX, treating the absorption and power-law index as free parameters. They derived best-fit parameters of  $N_H = 2.2 \times 10^{21}$   $cm^{-2}$  and  $\Gamma = 2.58$  for the second brightest source in NGC 3379, which accounts for

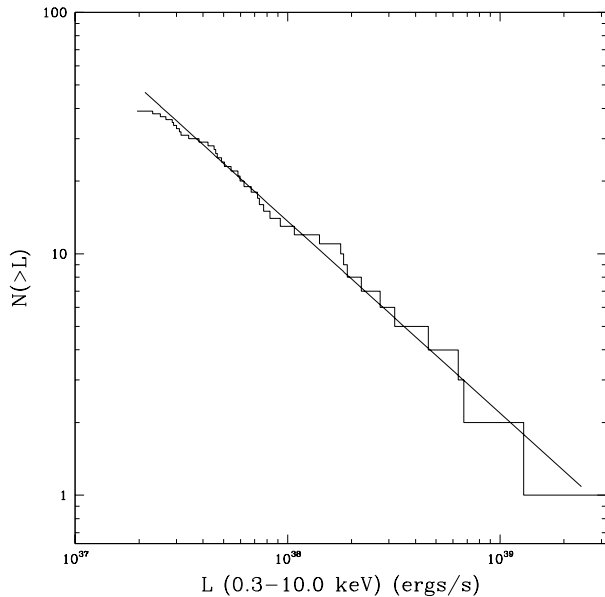


FIG. 3.— Cumulative luminosity function of all point sources detected within the central 5', excluding the central AGN. Also shown is the best-fit power law luminosity function for sources detected at greater than  $4\sigma$

much of the difference between our two luminosity estimates for the second brightest source in NGC 3379.

### 2.1. Luminosity Function and Spatial Distribution

Excluding the central AGN, there are 39 detected sources in the central 5 kpc of the galaxy (see the luminosity function in Fig. 3). We first fitted the luminosity function of all 39 sources using the maximum likelihood method in Crawford, Jauncey & Murdoch (1970) to a power-law model ( $N(>L) = kL^{-\alpha}$ ) and obtained a best-fit index of  $\alpha = 0.60 \pm 0.15$  ( $1\sigma$  error). This gives a reasonable fit at low fluxes, but significantly overestimates the number of brighter sources. We then repeated the analysis only including sources detected at more than  $4\sigma$  and obtained an acceptable fit with  $\alpha = 0.80 \pm 0.2$  (see Fig. 3). The luminosity function does not have a break near the Eddington-limit of a neutron star ( $L_{\text{edd}} = 1.6 \times 10^{38}$  ergs  $\text{cm}^{-2}$   $\text{s}^{-1}$ ) as observed in some early-type galaxies (Sarazin et al. 2001). The flattening of the luminosity function at low fluxes may be due to the presence of extended emission in the center of the galaxy which raises the detection threshold in this region.

Kim & Fabbiano (2004) recently derived the luminosity function for a sample of early-type galaxies, including NGC 3379, but they only included sources beyond the central  $20''$  and within the  $D_{25}$  ellipse ( $5.4'$  by  $4.8'$ ). However, they obtained a best-fit index of  $\beta = 1.8$  for the differential luminosity function, which corresponds to the same index we find for the cumulative luminosity function. Colbert et al. (2004) calculated the point source luminosity function in 23 late-type galaxies and 9 early-type galaxies, including NGC 3379. Fitting the luminosity function of the 12 sources with luminosities greater than  $10^{38}$  ergs  $\text{s}^{-1}$  and within the  $D_{25}$  ellipse, they obtained a best-fit index for the cumulative luminosity function of 1.07, which is consistent with our results within the errors. In general, star forming galaxies have flatter luminosity functions than early-type galaxies. For example, Colbert et al. find an average index for spiral and starburst galaxies of  $\alpha = 0.6 - 0.8$  compared to ellipticals with  $\alpha \approx 1.4$ . However, the average slope of the

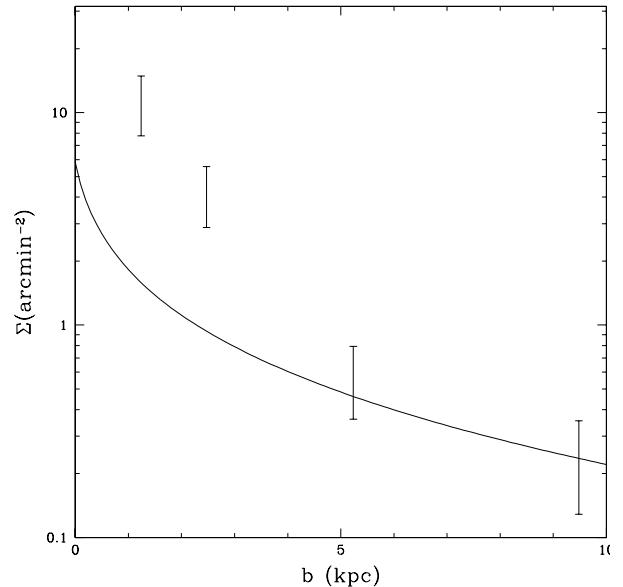


FIG. 4.— Surface brightness profile of the detected X-ray point sources in NGC 3379 along with the optical surface brightness profile (solid line). The normalization of the optical surface has been adjusted for comparison.

14 ellipticals analyzed in the Kim & Fabbiano (2004) sample is  $\alpha = 0.9$ , which is consistent with our result for NGC 3379.

While the ratio of the combined X-ray luminosity of the detected point sources in NGC 3379 to the optical luminosity of the galaxy is consistent with other early-type galaxies observed by Chandra (Colbert et al. 2004), the point sources have a much more centrally peaked surface brightness profile than the optical light of the galaxy (see Fig. 4). The optical surface brightness profile in Fig. 4 is based on the de Vaucouleurs profile for NGC 3379 found by Capaccioli et al. (1990) with  $r_e = 54.8''$  and  $\mu_e = 22.24$  mag  $\text{arcsec}^{-2}$ . For comparison, Finoguenov & Jones (2002) found that there was a deficit of detected point sources in the core of M84 compared to the optical surface brightness profile of the galaxy. However, there is significantly more diffuse emission in M84 compared to NGC 3379, and the deficit of point sources in the core may be due to the lower sensitivity of detecting point sources in the presence of diffuse emission. Accounting for the lower sensitivity of detecting point sources in the core of NGC 3379, would only increase the excess of point sources within the central few kpc.

### 2.2. Hardness Ratios

Of all the discrete sources in NGC 3379, only the ULX has sufficient counts for a detailed spectral analysis (see §3). To help in the identification of the detected point sources, we followed Prestwich et al. (2003) and extracted counts in a soft band from 0.3-1.0 keV, a medium band from 1.0-2.0 keV and a hard band from 2.0-8.0 keV. We then computed a soft X-ray color from  $(M-S)/T$  and a hard X-ray color from  $(H-M)/T$ , where T is the total number of counts in all 3 bands. The resulting color-color diagram for all non-nuclear sources detected at more than  $4\sigma$  and within the central 5 kpc is shown in Fig. 5. The circle in Fig. 5 delineates the color-color region associated with LMXBs determined by Prestwich et al. This figure shows that all of the sources detected in NGC 3379 have X-ray colors consistent with LMXBs. Thermal supernova remnants and

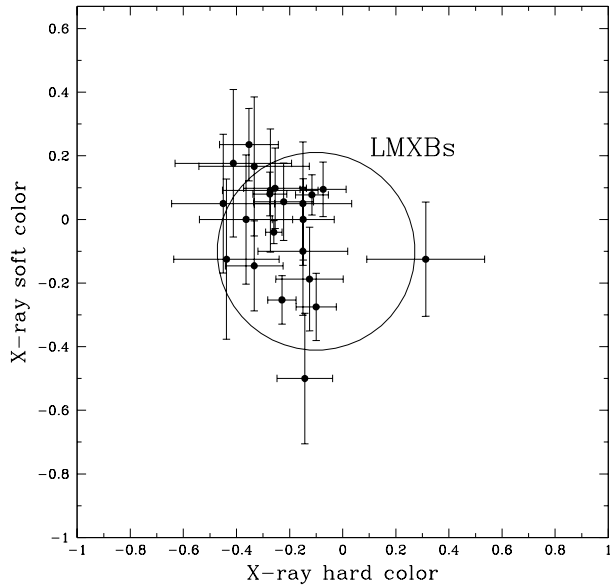


FIG. 5.— Color-color diagram for all non-nuclear point sources detected at more than  $4\sigma$  significance within the central 5 kpc. The circle shows the range of colors of LMXBs identified in Local Group galaxies.

super-soft sources have softer colors, while HMXBs typically have harder colors.

### 2.3. Fraction in Globular Clusters

Whitlock, Forbes & Beasley (2003) list the positions of 133 globular clusters in NGC 3379, of which 105 are within the S3 field-of-view. They find that the net surface brightness of globular clusters is consistent with zero beyond  $5.5'$  from the center of the galaxy which roughly corresponds to the farthest corner of the S3 chip. Of the 65 non-nuclear point sources detected in the S3 image, only 3 are within  $2''$  of the globular cluster positions in Whitlock et al. Fig. 6 shows shows the raw 0.3–6.0 keV S3 data for the central 10 kpc by 10 kpc region of NGC 3379, along with  $2''$  radius circles at the globular cluster positions. Within the central 5 kpc, only 2 (identified as S1 and S2 in Fig. 6), of the 39 non-nuclear point sources are coincident with globular clusters. This figure shows that the globular cluster sample is highly incomplete within the central  $20''$  due to the difficulty of detecting globulars against the brightest parts of the galaxy. However, even if we exclude the central  $20''$  and consider only the remaining 25 point sources within the central 5 kpc, only 2 (8%) of these sources are identified with globular clusters. This is significantly less than the 50% typically found in early-type galaxies (Sarazin et al. 2003). The X-ray luminosity threshold in our observation is  $2.2 \times 10^{37}$  ergs  $s^{-1}$ , which is fainter than that in most other studies of the binary populations in early-type galaxies, so incompleteness in the X-ray point source sample should not be a factor. Kundu & Whitmore (2001) find that the turnover absolute magnitude of the globular cluster luminosity function for a sample of early-type galaxies, including NGC3379, is  $M_v = -7.41$ . The lower magnitude cut in the Whitlock et al. globular cluster sample is  $m_B = 23$ , corresponding to  $m_v \approx 22.3$  for NGC 3379. Using the distance modulus for NGC 3379, the turnover magnitude in the globular cluster luminosity function should be  $m_v^0 \approx 22.7$ , which is slightly fainter than the magnitude cut in the Whitlock et al. sample. Thus, incompleteness in the globular cluster sample

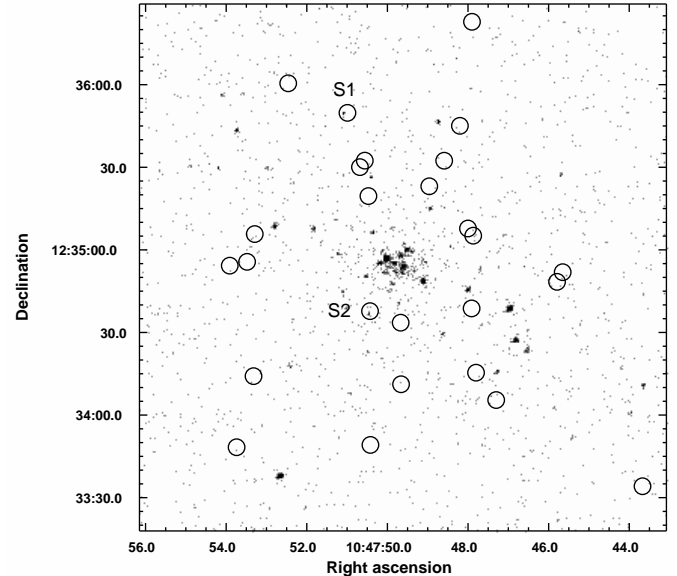


FIG. 6.— The raw 0.3–6.0 keV S3 image of NGC3379. The image is 10 kpc on a side. Also shown are the locations of the globular clusters from Whitlock, Forbes & Beasley (2003). Only two X-ray point sources, labeled S1 and S2, are within  $2''$  of the globular cluster positions.

should not have a significant impact on the small fraction of X-ray point sources associated with globular clusters in NGC 3379, especially since Sarazin et al. (2003) find that X-ray point sources in early-type galaxies tend to be found in the optically more luminous globular clusters.

NGC3379 has a very low specific frequency of globular clusters for an elliptical galaxy,  $S_N = 1.2$  (Kundu & Whitmore 2001), which is equal to the mean found for a sample of Sa and Sb galaxies (Harris 1991). There is some evidence that the fraction of X-ray point sources associated with globular clusters increases from late to early-type galaxies (Sarazin et al. 2003). The fraction in NGC 3379 is actually consistent with our Galaxy, within which approximately 10% of LMXBs are associated with globular clusters (White, Nagase & Van den Heuvel 1995). It is interesting to note that there has been significant debate over the years whether NGC 3379 is an elliptical or a low inclination S0 galaxy as suggested by Capaccioli et al. (1990). The low specific frequency of globular clusters in NGC 3379 and the small fraction of X-ray point sources associated with globular clusters are consistent with the Chandra observation of the S0 galaxy NGC 1553 (Blanton, Sarazin & Irwin 2001).

### 3. ULX SPECTRA AND LIGHTCURVE

The brightest source in NGC 3379 (labeled ULX in Fig. 1) is located approximately  $7''$  (360 pc) to the NE of the AGN. This source is not in a known globular cluster, but it is difficult to detect globulars so close to the galactic center. We extracted a spectrum of this source using the region generated by *wavdetect* which is approximately the 90% encircled energy aperture at 1 keV. A background spectrum was acquired from within the central  $10''$  region of the galaxy after excising all emission from detected point sources. We first fitted the 0.3 to 3.0 keV spectrum with an absorbed multi-color disk (MCD) blackbody model, but the fit was unacceptable ( $\chi^2/\text{DOF} = 38/28$ ). We then tried an absorbed power-law model and obtained an acceptable fit ( $\chi^2/\text{DOF} = 27.8/28$ ) with  $\Gamma = 1.6 \pm 0.3$  (90% confidence

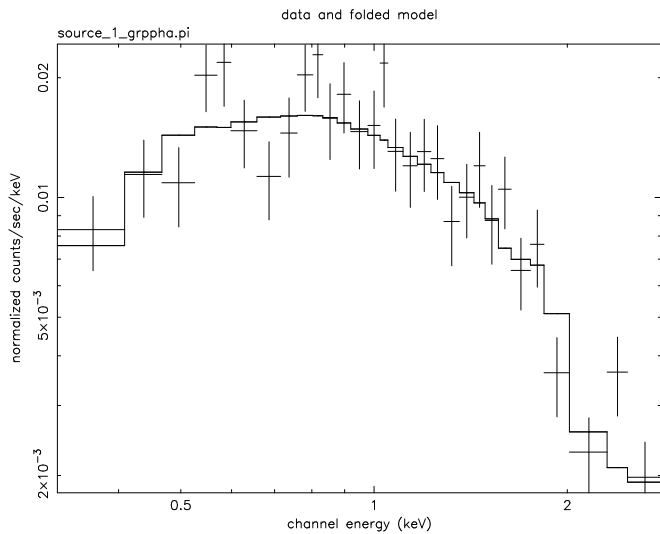


FIG. 7.— ACIS-S3 spectrum of the ULX along with the best-fit absorbed power-law model.

limit) and galactic absorption (see Fig. 7). Adding a disk component to the power-law model did not improve the fit further. The unabsorbed 0.3-10.0 keV flux is  $2.0 \times 10^{-13}$  ergs  $\text{cm}^{-2}$   $\text{s}^{-1}$ , which corresponds to  $L(0.3-10.0 \text{ keV}) = 2.7 \times 10^{39}$  ergs  $\text{s}^{-1}$ . The probability of detecting a background source with a flux equal to, or greater than this value within the central  $7''$  of the galaxy is less than  $10^{-4}$ .

The intensity of this source varies smoothly by a factor of two during the course of the 30 ksec observation (see Fig. 8). The peak luminosity of the source is  $3.5 \times 10^{39}$  ergs  $\text{s}^{-1}$  which places it among the ULX class of objects and corresponds to the Eddington luminosity of a  $30M_{\odot}$  black hole. We also generated a hardness ratio light curve, but did not find significant variations during the observation.

To check for long-term variability in the ULX, we examined the 24 ksec ROSAT HRI observation of NGC 3379 taken on Aug. 2, 1996 and found that the X-ray emission was centered on the ULX, not the center of the galaxy. The net HRI count rate within a  $10''$  radius aperture (corresponding to the 90% encircled energy radius) centered on the J2000 coordinates of the ULX as determined from the S3 image is  $3.3 \times 10^{-3}$  ct  $\text{s}^{-1}$ . Assuming an absorbed power-law model with the best-fit parameters listed above gives an unabsorbed 0.3-10.0 keV flux of  $3.0 \times 10^{-13}$  ergs  $\text{cm}^{-2}$   $\text{s}^{-1}$ , which is 50% higher than the ACIS measured flux of the ULX in 2001. The HRI flux measurement is undoubtedly affected by contamination from other point sources. Based on the S3 image, the ULX contributes 60% of the flux within the same aperture used to compute the HRI flux. Thus, there is strong evidence that the ULX was at a comparable luminosity 5 years prior to the Chandra observation. There are insufficient counts in the HRI data to measure short term variability.

#### 4. DIFFUSE EMISSION AND THE AGN

After excising the emission from all detected point sources, we extracted a spectrum of the diffuse emission within the central  $15''$  ( $770 \text{ pc}$ ). A background spectrum was taken from a circular aperture  $2.5'$  from the center of the galaxy on the S3 chip. The background subtracted spectrum was then fitted to an absorbed thermal (MEKAL) plus power-law model in the 0.3-5.0 keV band. The best-fit power-law component has

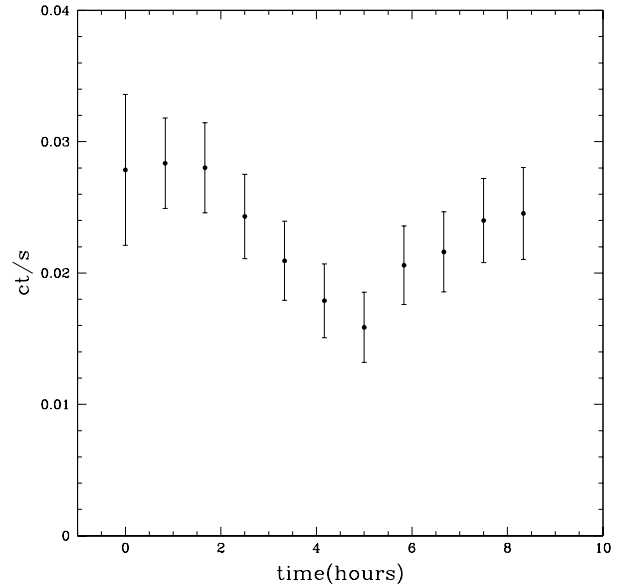


FIG. 8.— The light curve of the ULX in the 0.3-6.0 keV band from the Chandra observation of 13 Feb, 2001. The data are binned into 3 ksec intervals.

$\Gamma = 1.7 \pm 0.3$  and an unabsorbed 0.3-10.0 keV flux of  $5.5 \times 10^{-14}$  ergs  $\text{cm}^{-2}$   $\text{s}^{-1}$ , corresponding to  $L(0.3-10.0 \text{ keV}) = 7.4 \times 10^{38}$  ergs  $\text{s}^{-1}$ . The best-fit thermal component has  $kT = 0.6$  (0.4-1.0 keV) and an unabsorbed 0.3-10.0 keV flux of  $6.6 \times 10^{-15}$  ergs  $\text{cm}^{-2}$   $\text{s}^{-1}$ , corresponding to  $L(0.3-10.0 \text{ keV}) = 8.9 \times 10^{37}$  ergs  $\text{s}^{-1}$ . All errors are given at the 90% confidence limit. This analysis shows that 90% of the remaining diffuse emission most likely arises from point sources with fluxes below the detection limit in the Chandra observation. Assuming the luminosity function derived above is valid at lower luminosities, then the luminosity of the unresolved power-law component can be generated by approximately 40 sources below  $3.0 \times 10^{37}$  ergs  $\text{s}^{-1}$ .

Using the best-fit emission measure in the thermal model and assuming a uniform gas distribution in the central  $770 \text{ pc}$  gives an electron number density of  $n_e = 0.01 \text{ cm}^{-3}$ , a gas mass of  $5 \times 10^5 M_{\odot}$ , and a cooling time ( $t_c = 5kTM_{\text{gas}}/2\mu m_p L$ ) of  $8 \times 10^8 \text{ yr}$ . If the gas is able to cool unimpeded, this gives a mass cooling rate within the central  $770 \text{ pc}$  of  $\dot{M} = 6 \times 10^{-4} M_{\odot} \text{ yr}^{-1}$ . The estimated central gas density in NGC 3379 is a factor of 10 less than that found in X-ray luminous ellipticals whose emission is dominated by hot gas (e.g., Lowenstein et al. 2001).

The optical luminosity density in NGC3379 can be determined from the surface brightness profile and Abel's formula (Binney & Tremaine 1987). Using the de Vaucouleurs profile for NGC 3379 found by Capaccioli et al. (1990), gives  $L_B = 2.3 \times 10^9 L_{\odot B}$  within the central  $770 \text{ pc}$ . Using the stellar mass loss rate from Faber & Gallagher (1976) for elliptical galaxies of  $0.15 M_{\odot} / (10^{10} L_{\odot} \text{ yr})$ , gives a stellar mass loss rate of  $\dot{M}_s = 0.035 M_{\odot} \text{ yr}^{-1}$ . Thus, the presently observed gas mass in NGC 3379 can be produced by stars in only  $10^7$  years, which is significantly less than the cooling time, and only 5 times the sound crossing time in this region. The continuous injection of gas shed by evolving stars with a temperature equal to the virial temperature of the stellar system essentially negates the effects of radiative cooling. Such a small amount of gas implies that most of the mass shed by stars has either been accreted by the central supermassive black hole or has been expelled from the central region in a wind.

The point source labeled AGN in Fig. 1 is located within  $1''$  of the optical centroid of the galaxy, and is probably associated with the central supermassive black hole with a dynamically measured mass of  $1.0 - 3.9 \times 10^8 M_\odot$  (Magorrian et al. 1998, Haring & Rix 2004). The central black hole in NGC3379 is also a weak 1.4 GHz radio source with a luminosity of  $\nu L_\nu = 4.3 \times 10^{35} \text{ ergs s}^{-1}$  (Condon et al. 1998). There are too few net counts in the S3 data to fit the spectrum of the AGN, but assuming an absorbed power-law model with  $\Gamma = 1.6$  and galactic absorption gives  $L(0.3-10.0 \text{ keV}) = 8.0 \times 10^{38} \text{ ergs s}^{-1}$ , corresponding to  $\sim 3 \times 10^{-8}$  of its Eddington limit. Using the density and temperature of the ambient gas derived above gives an accretion radius for the central black hole of  $R_a = GM_{bh}/c_a^2 = 7 \text{ pc}$ , and a Bondi accretion rate  $\dot{M}_b = 4\pi R_a^2 \rho_g c_a = 6 \times 10^{-5} M_\odot \text{ yr}^{-1}$ , which is a factor of 10 below the cooling rate within the central 770 kpc. The implied efficiency,  $\epsilon = L/\dot{M}c^2$ , of the central AGN assuming Bondi accretion is  $2 \times 10^{-6}$ . This low efficiency is typical of that found for supermassive black holes at the centers of ellipticals (Lowenstein et al. 2001, DiMatteo et al. 2003). The low luminosity of the central black holes in ellipticals can be explained by either a very low radiative efficiency, as in the advection dominated accretion flow model (ADAF; Narayan & Yi 1994) or radiatively inefficient accretion flow model (RIAF; Yuan & Narayan 2005), or a reduction in the accretion rate, as in models with both inflow and AGN driven outflows (e.g., Blandford & Belgelman 1999).

While the uncertainty on the temperature of the diffuse gas is large, the best-fit temperature is twice the temperature associated with the velocity dispersion of the stars ( $kT = \mu m_p \sigma_p^2 / k = 0.3 \text{ keV}$  for  $\sigma_p = 217 \text{ km s}^{-1}$ ; Prugniel & Simien 1996). This suggests that the gas is being heated by the central AGN and is presently flowing out of the system in a galactic wind. Assuming the gas is in a steady-state wind (i.e.,  $\dot{M}_s = 4\pi r^2 \rho_g u_w$  at 770 pc) gives  $u_w = 20 \text{ km s}^{-1}$  and an energy outflow rate (mostly thermal) of  $5 \times 10^{39} \text{ ergs s}^{-1}$ , which is 4 orders of magnitude greater than the radio luminosity of the AGN. The low wind velocity near the galactic center is typical of galactic wind models since the wind velocity continues to increase with increasing radius (e.g., David, Forman & Jones 1991). The lack of detectable diffuse emission at large radii in NGC 3379 may be due to the greater wind velocities and lower gas densities.

Chandra has detected X-ray cavities filled with radio emitting plasma and AGN driven shocks in many cluster cooling flows and individual elliptical galaxies (e.g., McNamara et al. 2000, Finoguenov & Jones 2002, Fabian et al. 2003, Blanton et al. 2003, Forman et al. 2005, Nulsen et al. 2005a, Nulsen et al. 2005b, McNamara et al. 2005). Based on the analysis of cavities found in a sample of 16 clusters, one group and one galaxy, Birzan et al. (2004) found that the ratio of mechanical to radio power of the central AGN varies from 10 in the most radio luminous AGNs, up to  $10^4$  in systems with less radio luminous AGNs. In clusters with AGN driven shocks, the shock energies are typically a few times the energy in the cavities, which further increases the ratio of mechanical to radio power. The largest shock and cavity energies yet observed are found in MS0735.6+7421 (McNamara et al. 2005), which has a ratio between mechanical and radio power of  $10^5$ . Thus, at least on energetics grounds, the hypothesis that the lack of a significant reservoir of hot gas in NGC 3379 is due to an AGN driven wind is consistent with Chandra observations of systems perturbed by radio outbursts. The low luminosities of the central supermassive black holes in ellipticals may, in general, arise

from the same feedback mechanism between the central AGN and hot gas as that observed in cluster cooling flows.

## 5. THE NATURE OF THE ULX

Based on ROSAT and Chandra observations, approximately 50% of late-type galaxies and less than 10% of early-type galaxies contain ULXs (Ptak & Colbert 2004, Irwin et al. 2004). In late-type galaxies, the ULXs are primarily associated with regions of star formation, indicating that they are most likely black hole binaries (BHBs) with high-mass companions. However, Colbert et al. (2004) recently estimated that 20% of the ULXs in spirals are not associated with recent star formation and could have low mass companions as is likely in early-type galaxies. As noted in the introduction, ULXs could arise from non-isotropic, sub-Eddington emission from stellar mass black holes, super-Eddington emission from stellar mass black holes, or sub-Eddington emission from IMBHs. van der Marel (2003) has noted that the X-ray luminosity function of X-ray point sources in galaxies can be fit by a single power-law, even to luminosities above  $10^{39} \text{ ergs s}^{-1}$ , suggesting that the accreting objects in ULXs are not a separate class of objects (e.g., IMBHs). There are 18 BHBs in our Galaxy with dynamically measured black hole masses between  $M_{bh} = 3 - 18 M_\odot$  (McClintock & Remillard 2004). Assuming isotropic emission, 3 of these binaries are super-Eddington, with peak luminosities up to 7 times their Eddington-limit, suggesting that some of the extragalactic ULXs could be stellar mass black holes. King (2003) has proposed that ULXs comprise two separate classes of super-Eddington mass accretion rate systems. In regions of recent star formation in spiral galaxies, ULXs would arise from thermal-timescale mass transfer in high mass X-ray binaries, while in elliptical galaxies, the ULXs would be similar to the micro-quasars observed in our galaxy. The long term stability of the ULX in NGC 3379 as determined from the ROSAT HRI and Chandra observations, may pose a problem for the micro-quasar interpretation of ULXs in early-type galaxies.

The mass of the central compact object in a ULX can be estimated, if thermal emission from an accretion disk can be detected, since the temperature at the inner edge of an accretion disk scales as  $T_{in} \propto M_{bh}^{1/4}$ . Spectral analysis of ASCA data on ULXs indicated that these objects could be described by the MCD model with inner disk temperatures of  $kT = 1.1 - 1.8 \text{ keV}$ , implying stellar masses for the accreting objects (Makishima et al. 2000). More recent analysis of Chandra and XMM-Newton data, however, indicate that some ULXs can be described as pure power-laws with  $\Gamma = 1.5 - 2.2$ , while others require a power-law plus disk model (e.g., Roberts et al. 2001, Zezas et al. 2002a, Zezas et al. 2002b, Humphrey et al. 2003, Miller et al. 2004, Liu, Bregman & Seitzer 2002). Soft accretion disks have been detected in two ULXs in NGC 1313 with inner disk temperatures of 150 eV, implying masses of  $100 - 1000 M_\odot$  (Miller et al. 2003). While we cannot estimate the black hole mass in the ULX in NGC 3379 due to the lack of detectable thermal emission from the disk, the best-fit power-law index ( $\Gamma = 1.7$ ) is consistent with recent Chandra and XMM-Newton results and similar to the low hard state observed in galactic BHBs (McClintock & Remillard 2004).

The power-law spectrum of the ULX in NGC 3379 suggests that the emission is dominated by Compton up-scattering of soft disk photons in a optically thin corona. The variability in the light curve could arise from a partial eclipse or absorption by cooler material in the outer parts of the accretion disk. The slow

rise and fall times in the light curve (see Fig. 8), along with the lack of any variation in hardness ratio, suggest that the intensity variation is due to a partial eclipse of the extended coronal emission with a period of 8-10 hours. While variability on the scales of months to years is well known for ULXs, there are only a few published cases of periodic variability on the time scale of hours, all of which are in late-type galaxies (Sugiho et al. 2001, Circinus; Bauer 2001; M51 Liu et al. 2002; NGC 628; Liu et al. 2005). The ULX in NGC 3379 is the only known ULX in an early-type galaxy with possible periodic behavior in its light curve on the time scale of hours.

Orbital periods of 8-10 hr are very common for LMXBs (Verbunt 1993). Assuming that the secondary star is filling its Roche lobe and transferring mass to the primary, we can estimate the mass of the secondary. Using the expression for the Roche lobe radius from Paczynski (1967) and Kepler's law gives  $P = 8.9(R_2/R_\odot)(M_\odot/M_2)$  hr (Verbunt 1993). For main sequence stars  $(R_2/R_\odot) = (M_2/M_\odot)$ , indicating that if the period is 8-10 hr, then the secondary star is approximately a solar mass. The mass-radius relation for a He core burning star or a white dwarf predicts a much larger mass for the secondary which is unlikely in an early-type galaxy.

## 6. SUMMARY

The Chandra observation of the intermediate luminosity elliptical galaxy NGC 3379 shows that only a small fraction of the gas shed by evolving stars still resides within the hot ISM. A wavelet detection algorithm resolves 75% of the emission within the central 5 kpc into point sources. The luminosity function of the point sources detected at greater than  $4\sigma$  significance is consistent with that found for other ellipticals observed by Chandra (Kim & Fabbiano 2004). Unlike other ellipticals observed by Chandra, only 8% of the point sources are associated with globular clusters, which is comparable to the fraction of LMXBs in our galaxy. The low specific frequency of globular clusters and the low fraction of X-ray point sources associated with globular clusters in NGC3379 is actually more similar to Chandra observations of S0 galaxies rather than ellipticals (e.g., Blanton, Sarazin & Irwin 2001).

Spectral analysis of the unresolved emission within the central  $15''$  (770 pc) indicates that 90% of the emission probably arises from point sources with fluxes below the detection limit in the Chandra observation. If the luminosity function of the detected point sources is valid at lower luminosities, then the diffuse power-law emission can be accounted for by approximately 40 sources with luminosities below  $3.0 \times 10^{37}$  ergs  $s^{-1}$ .

The remaining 10% of the unresolved emission from the central 770 pc is well described by thermal emission with  $kT = 0.6$  keV. Assuming a uniform gas density in this region gives a gas mass of  $5 \times 10^5 M_\odot$ , which can be supplied by stellar mass loss in  $10^7$  years. Such a small amount of gas indicates that the stellar mass loss is either being expelled from the central regions in a wind or is being accreted by the central black hole. The X-ray luminosity of the central AGN is  $8 \times 10^{38}$  ergs  $s^{-1}$ . If gas is being accreted by the central black hole at either the Bondi accretion rate or mass cooling rate, then the radiative efficiency of the black hole must be  $\sim 10^{-6}$ , as in the ADAF or RIAF models (Narayan & Yi 1994 and Yuan & Narayan 1995). If the gas is flowing out of the system in a wind, the energy outflow rate would be  $5 \times 10^{39}$  ergs  $s^{-1}$ , which is 4 orders of magnitude greater than the 1.4 GHz radio power of the AGN. Such a large ratio between AGN mechanical and radio power is commonly found among cluster cooling flows with X-ray cavities and shocks (Birzan et al. 2004; Nulsen et al. 2005a; Nulsen et al. 2005b; McNamara et al. 2005).

The most luminous source in NGC3379 is located 360 pc from the central AGN with a peak luminosity of  $3.5 \times 10^{39}$  ergs  $s^{-1}$ , corresponding to the Eddington luminosity of a  $30M_\odot$  object. The spectrum of this source is well fitted with an absorbed power-law model with  $\Gamma = 1.7$ , which is similar to other ULXs observed by Chandra and XMM-Newton and the low-hard state of galactic black hole binaries. Examining the archival ROSAT HRI observation of NGC 3379 shows that the ULX was at a comparable luminosity 5 years prior to the Chandra observation. The long term stability of the ULX may pose a problem for the micro-quasar interpretation of ULXs in early-type galaxies.

The light curve of the ULX in NGC 3379 varies smoothly by a factor of two during the Chandra observation. The slow rise and fall times in the light curve and the consistency of the power-law spectrum during the observation all suggest that the ULX is undergoing a partial eclipse of the extended corona surrounding an accretion disk with a period of 8-10 hr. Assuming the secondary is a main sequence star filling its Roche lobe gives a mass for the secondary of approximately  $1M_\odot$ . Variability has been observed in other ULXs, but the ULX in NGC 3379 is the only ULX in an elliptical galaxy with possible periodic behavior. Due to the high surface brightness density of sources in the central 1 kpc of NGC 3379, only a long Chandra observation can determine if the lightcurve of the ULX is truly periodic.

## REFERENCES

- Angelini, L., Lowenstein, M. & Mushotzky, R. 2001, *ApJ*, 557, L35.  
 Bauer, F. et al. 2001, *ApJ*, 122, 182.  
 Begelman, M. 2002, *ApJ*, 568, L97.  
 Binney, J. & Tremain, S. 1987, in *Galactic Dynamics*, (Princeton University Press: Princeton).  
 Birzan, L., Rafferty, D., McNamara, B., Wise, M. & Nulsen, P. 2004, *ApJ*, 607, 800.  
 Blandford, R. & Begelman, M. 1999, *MNRAS*, 303, L1.  
 Blanton, E., Sarazin, C. & Irwin, J. 2001, *ApJ*, 552, 106.  
 Blanton, E., Sarazin, C. & McNamara 2003, *ApJ*, 585, 227.  
 Capaccioli, M., Held, E., Lorenz, H. & Vietri M. 1990, *AJ*, 99, 1813.  
 Colbert, E., Heckman, T., Ptak, A., Strickland, D. Weaver, K. 2004, *ApJ*, 602, 231.  
 Condon, J. Cotton, W., Greisen, E., Yin, Q., Perley, R., Taylor, G. & Broderick, J. 1998, *AJ*, 115, 1693.  
 Crawford, D., Jauncey, D. & Murdoch, H. 1970, *ApJ*, 162, 405.  
 David, L., Forman, W. & Jones, C. 1991, *ApJ*, 369, 121.  
 DiMatteo, T., Allen, S., Fabian, A. & Wilson, A. 2003, *ApJ*, 582, 133.  
 Faber, S. & Gallagher, J. 1976, *ApJ*, 204, 365.  
 Fabian, A., Sanders, J., Allen, S., Crawford, C., Iwasawa, K., Johnstone, R., Schmidt, W. & Taylor G. 2003, *MNRAS*, 344, 43.  
 Ferrarese, L., et al. 2000, *ApJ*, 529, 745.  
 Finoguenov, A. & Jones, C. 2002, *ApJ*, 574, 754.  
 Forman, W., Jones, C. & Tucker, W. 1985, *ApJ*, 293, 102.  
 Forman, W., Nulsen, P., Heinz, S., Owen, F., Eilek, J., Vikhlinin, A., Markevitch, M., Kraft, R., Churazov, E., Jones C. 2005 (astro-ph/0312576).  
 Giacconi, R., Rosati, P., Tozzi, P., Nonino, M., Hasinger, G., Norman, C., Bergeron, J., Borgani, S., Gilli, R., Gilmozzi, R., Zheng, W. 2001, *ApJ*, 551, 624.  
 Haring, N. & Rix, H. 2004, *ApJ*, 604, L89.  
 Harris, 1991, *W. ARAA*, 29, 543.  
 Humphrey, P., Fabbiano, G., Elvis, M., Church, M. & Balucinska-Church, M. 2003, *MNRAS*, 344, 134.  
 Irwin, J., Bregman, J. & Athey, A. 2004, *ApJ*, 601, L143.  
 Jeltema, T., Canizares, C., Buote, D. & Garmire, G. 2003, *ApJ*, 585, 756.  
 Kim, D., Fabbiano, P. & Trinchieri, G. 1992, *ApJ*, 393, 134.

- Kim, D. & Fabbiano, G. 2004, *ApJ*, 611, 846.
- King, A. Davies, M., Ward, M., Fabbiano, G. & Elvis, M. 2001, *ApJ*, 552, L109.
- King, A. 2003, *MNRAS*, 335, L13.
- Kraft, R. et al. 2001, *ApJ*, 560, 675.
- Liu, J., Bregman, J. Irwin, J. & Seitzer, P. 2002, *ApJ*, 581, L93.
- Liu, J., Bregman, J., Lloyd-Davies, E., Irwin, J., Espaillat, C., Seitzer, P. 2005, *ApJ*, 621, L17.
- Kundu, A. & Whitmore, B. 2001, *AJ*, 121, 2950.
- Lowenstein, M., Mushotzky, R., Angelini, L., Arnaud, K. & Quataert, E. 2001, *ApJ*, 555, 21L.
- Makishima, K., Kubota, A., Mizuno, T., Ohnishi, T., Tashiro, M., Aruga, Y., Asai, K., Dotani, T., Mitsuda, K., Ueda, Y., Uno, S., Yamaoka, K., Ebisawa, K., Kohmura, Y., Okada, K. 2000, *ApJ*, 535, 632.
- Macchetto, F., Pastoriza, M., Caon, N., Sparks, W., Giavalisco, M., Bender, R., Capaccioli, M. 1996, *A&AS*, 120, 463.
- Magorrian, J., Tremaine, S., Richstone, D., Bender, R., Bower, G., Dressler, A., Faber, S., Gebhardt, K., Green, R., Grillmair, C., Kormendy, J., Lauer, T. 1998, *AJ*, 115, 2285.
- McClintock, J. & Remillard, R. 2004, in "Compact Stellar X-ray Sources," eds. W.H.G. Lewin and M. van der Klis, (Cambridge:Cambridge University Press).
- McNamara, B., Wise, M., Nulsen, P. E. J., David, L., Sarazin, C., Bautz, M., Markevitch, M., Vikhlinin, A., Forman, W., Jones, C., Harris, D. 2000, *ApJ*, 534, 135.
- McNamara, B., Nulsen, P., Wise, M., Rafferty, D., Carilli, C., Sarazin, C. & Blanton, E. 2005, *Nature*, 433, 45.
- Miller, J., Fabbiano, G., Miller, M. & Fabian, A. 2003, *ApJ*, 585, L37.
- Miller, J., Zezas, A., Fabbiano, G. & Schweizer, F. 2004, *ApJ*, 609, 728.
- Narayan, R. & Yi, L. 1994, *ApJ*, 428, L13.
- Nulsen, P., McNamara, B., Wise, M. & David, L. 2005a, (astro-ph 0408315).
- Nulsen, P., Hambrick, D., McNamara, B., Rafferty, D., Birzan, L., Wise, M. & David, L. 2005b, (astro-ph 0504350).
- Paczynski, B. 1967, *Acta Aston*, 17, 287.
- Pastoriza, M., Winge, C., Ferrari, F., Macchetto, F., Caon, N. 2000, *ApJ*, 529, 826.
- Prestwich, A., Irwin, J., Kilgard, R., Krauss, M., Zezas, A., Primini, F., Kaaret, P. & Boroson, B. 2003, *ApJ*, 595, 719.
- Prugniel, Ph. & Simien, F. 1996, *AA*, 309, 749.
- Ptak, A. & Colbert, E. 2004, *ApJ*, 2004, 606.
- Roberts, T., Goad, M., Ward, M., Warwick, R., O'Brien, P., Lira, P., Hands, A. 2001, *MNRAS*, 325, L7.
- Sarazin, C., Irwin, J. & Bregman, J. 2001, *ApJ*, 556, 533.
- Sarazin, C., Kundu, A., Irwin, J., Sivakoff, G., Blanton, E., Randall, S. 2003, *ApJ*, 595, 743.
- Statler, T. 2001, *AJ*, 121, 244.
- Sugih, M, Kotoku, J., Makishima, K., Kubota, A., Mizuno, T., Fukuzawa, Y., Tashiro, M. 2001, *ApJ*, 561, L73.
- Swartz, D., Ghosh, K., Tennant, A. & Wu, K. 2004, *ApJ Supl.*, 154, 519.
- Terlevich, A. & Forbes, D. 2002, *MNRAS*, 330, 547.
- Tonry, J. et al. 2001, *ApJ*, 546, 681.
- van der Marel, R. 2003, in *Carnegie Observatories Astrophysics Series, Vol. 1: Coevolution of Black Holes and Galaxies*, ed. L. C. Ho, (Cambridge:Cambridge University Press), 37.
- van Dokkum, P. & Franx, M. 1995, *AJ*, 110, 2027.
- Verbunt, F. 1993, *ARAA*, 31, 93.
- White, N., Nagase, F. & Parmar, A. 1995, in *X-ray binaries*, ed. W. Lewin, J. van Paradijs & E. van den Heuvel. (Cambridge:Cambridge University Press), 1.
- Whitlock, S., Forbes, D. & Beasley, M. 2003, *MNRAS*, 345, 949.
- Yuan, F. & Narayan, R. 2005, *ApJ*, 612, 724.
- Zezas, A., Fabbiano, G., Rots, A. & Murray, S. 2002b, *ApJ Suppl*, 142, 239.
- Zezas, A., Fabbiano, G., Rots, A. & Murray, S. 2002b, *ApJ*, 577, 710.